

Figure 11: The physiological status of a person per minute; below, the rest of variables.

parameters indicating energy seem to rise at first, maintain a constant, medium level afterwards, and finally start decaying, probably due to the continuous effort that the patient is exerting.

In Fig. 10, we can readily see how the HR is constantly increasing, be it due to stress, attention or both, and reaches maximum values at the last minutes of the test. However, the RR is not always kept at high levels. RR seems to increase at first, which suggests, along with a high HR, that our patient might be stressed but then decreases, while RR simultaneously increases, as well as SCL, which can be a clear sign of attention, since the patient might be focusing harder on the task. Just after that, especially in the last minutes as we approach the end of the test, HR decreases and both components of GSR decrease, as opposed to what would be expected from attention moments. This might be an indication of fatigue, which is also observable in Fig. 11 by a decrease in energy levels.

4 Anthropometry

Anthropometry refers to the measurement of the human individual. In Section 4.1, we present the variables and parameters used. In Section 4.2, we describe the theory from what could be real-life case. We will be studying, within Section 4.3, the mathematical analysis to implement these parameters. In Section 4.4 we study the COM path for different velocities and derive an inference from the different patterns that appear. In Section 4.5, we show the motion of a person -that is simply walking- through the theoretical concepts derived from the aforementioned sections. Furthermore, we will be emulating the body motion in the MATLAB environment.

4.1 Variables and parameters

There are a set of variables or parameters that must be defined in the MATLAB script and are obtained from the table studied in Anthropometry theory (2).

In order to carry out the mathematical computations in Section 4.3, we will need the variables from the table in the Anthropometry theory (2). Specifically, we will need $\alpha_M = 0.061$, from which we will be able to obtain the mass $M_g = M \cdot \alpha_M$, used in later sections. Also note that the gravity is commonly expressed as $g = 9.81$ and the length of the table as $l = 2$.

4.2 Environment and theory

A man is seated in a fixed spot, his legs hanging in the air. A sensor is above its ankle, recording motion in the x direction, and a mass is attached to its ankle by a system of pulleys. Θ is the angle of its leg; x , the displacement.

Patient's initial position is as illustrated in Figure 14. The weight attached to the patient's ankle by a system of pulleys is pulling his leg forward. The leg is, at first, pushed backwards and, then, left free.

As shown in Figure 14 (Right), we compute all parameters in the *leg* system from the values shown in the left-hand side of the equations, namely b , l_g , l_1 and l_2 .

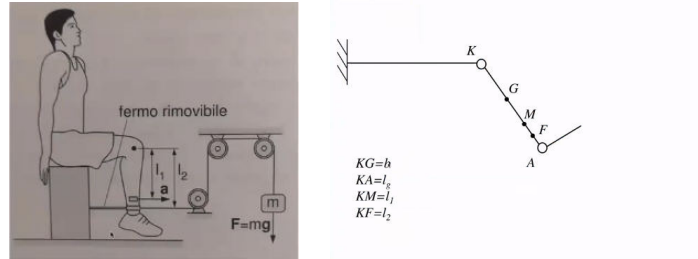


Figure 12: Patient's initial position (Left) and the schematic representation of the leg as a system (Right).

In a second experiment, a man is laying down on a 2m table, as shown in Fig. 13.

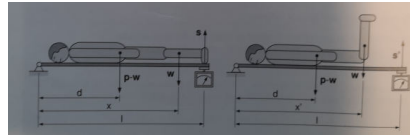


Figure 13: Patient's initial position (Left), laying face-down on a table, and same patient lifting their feet (Right).

4.3 Mathematical Analysis

In this section, we describe all the mathematical procedures for both the anthropometry study (first sub-section), and software emulation (later sub-sections).

4.3.1 Anthropometry experiment

We use our theory knowledge from Reference (2) to compute the unknown parameters, specifically ρ . Note that, in order to find such parameter, we must first carry out the following operations to find the required variables that will lead us towards ρ .

$$l_p = m \cdot l_2. \quad (2)$$

$$\rho_p = \sqrt{\frac{l_p}{M_g}} \quad (3)$$

From Eq. 2 we can find ρ_p in Eq. 3. Then we find the regression line for l_g and ρ_p . Similarly, we use equation 5 to find l_b , aided by Eqs. 4 and 6.

$$b = (s - s') \cdot \frac{l}{W} \quad (4)$$

$$l_b = l_p - M_g \cdot b^2 \quad (5)$$

$$\rho_b = \sqrt{\frac{l_b}{M_g}} \quad (6)$$

Once again, we find, in the same manner as before, Eq. 7 with the help of Eq. 8, for the distal components.

$$l_d = l_p + M_g \cdot (l_g - b)^2 \quad (7)$$

$$\rho_d = \sqrt{\frac{l_d}{M_g}} \quad (8)$$

Finally, we compute the regression between I_g and the different ρ values, namely, ρ_p , ρ_b , ρ_d , as shown in Fig. 15.

4.3.2 Center Of Mass

Throughout the experiment, we must compute the center of mass between several parts of our body, where our markers are placed, for instance, feet at the bottom, or trochanters in the femur. We can do so by means of Eq. 9.

$$marker_p \cdot (1 - b) + marker_d \cdot b \quad (9)$$

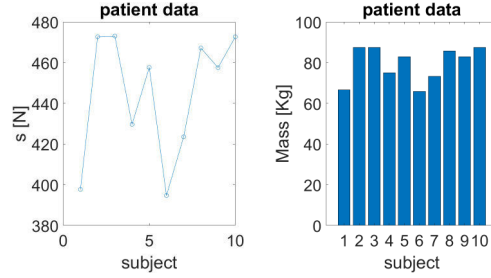


Figure 14: Patient's data used in mathematical step in Section 4.3. S on the right and Mass on the Right.

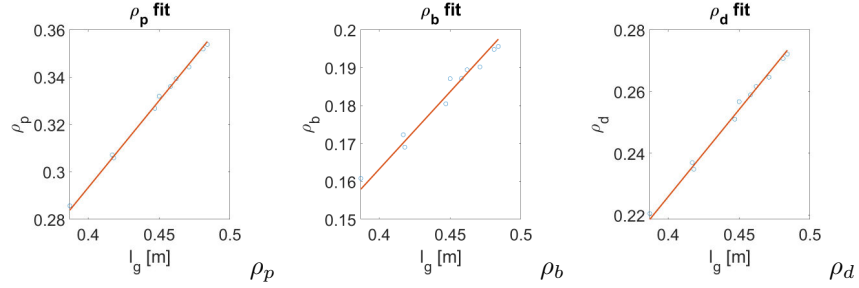


Figure 15: Linear regression models for each ρ value.

Also note that we might need to hypothesize to find some in-between markers. For example, the pelvis will be in the middle of each throcanter, but L4 (lumbar region, 4th vertebrae) will be found between C7 (cervical region, 7th vertebrae) and the pelvis.

4.3.3 Total Center Of Mass

The total center of mass is computed by multiplying each center of mass by the mass corresponding to such segment. It must be divided by the mass of the patient. Note that each leg must be considered twice, while pelvis or thorax, just once. Such equation is described in Eq. 10.

$$A = com_{RT} \cdot m.T + com_{RS} \cdot m.S + com_{RF} \cdot m.F + com_{LT} \cdot m.T$$

$$B = com_{LS} \cdot m.S + com_{LF} \cdot m.F + com_{TA} \cdot m.TA + com_P \cdot m.P$$

$$\frac{A + B}{2 \cdot m.T + 2 \cdot m.S + 2 \cdot m.F + m.TA + m.P} \quad (10)$$

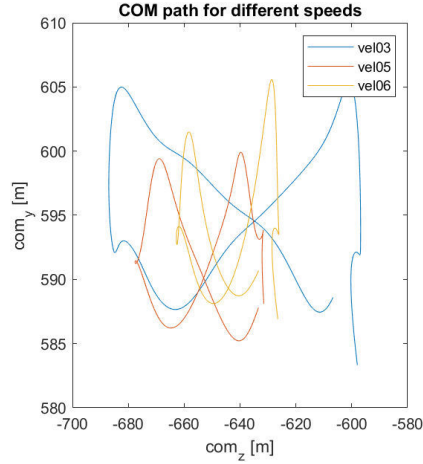


Figure 16: COM paths for different speeds.

4.4 Conclusions

Regarding the last experiment, conducted on MatLab, we can study the Center of mass (COM) path in coronal plane (X-Z) across range of walking speeds.

With such aim, we shall plot the different COM paths for the different speeds, as shown in Fig. 16. It is observable that the COM path seems to follow an infinite-shaped (∞) pattern, especially for v03. We can also appreciate from the same figure that, as the speed increases, so does the pattern become more U-shaped, more flagrantly in v06 (10). Mathematically, the values in which the Z axis ranges is $(-686.9, -596.8)$, $(-677.6, -631.5)$, $(-662.8, -626.1)$, for v03, v05 and v06, respectively. Clearly, the range of values reduces as the speed increases. In the Y axis, however, repeating analogously the mathematical steps, we obtain $(583.3, 605.3)$, $(585.2, 599.9)$, $(586.9, 605.6)$. In this case we can deduce that increasing the speed does not significantly reduce the range of values on the Y axis. Thus, reducing the values on the Z axis but maintaining constant those in the Y axis, the COM path patter goes from a infinite shape to a U-ish shape.

4.5 MATLAB emulation

In this section, we present some of the photo-frames of our MATLAB-based software emulation. The script was built from the theoretical concepts described above but, obviously, a skilled software implementation is required to take it to practice, as shown in Figure 17.

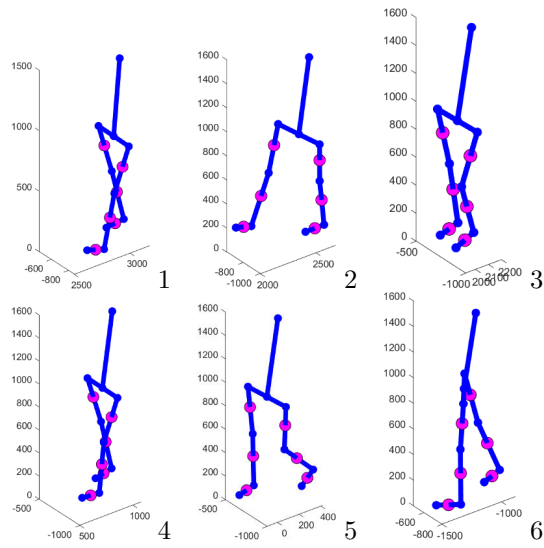


Figure 17: Several ordered, random photo-frames from the MATLAB software emulation.